SUPPLEMENTARY INFORMATION INVENTORY

Figure S1 – related to Figure 1: *Rspo3* from the outer adrenal capsule is the main source of R-spondins in the adrenal gland. This figure provides single-molecule *in situ* hybridizations (ISHs) for each R-spondin family member in 6-week-old mice showing that *Rspo3* is the most highly expressed.

Figure S2 – related to Figure 2: Male *Znrf3* cKO mice are histologically similar to female cKOs. This figure provides gross histology, adrenal weight measurements, and H&E images from male cKO mice showing that the phenotype of ZNRF3 loss is similar in male and female mice at 6 weeks of age.

Figure S3 – related to Figure 2: *Rnf43* does not compensate for *Znrf3* loss in the adrenal cortex. This figure provides single-molecule ISHs for *Rnf43* in control and *Znrf3* cKO mice and demonstrates that *Rnf43* expression is not induced with loss of ZNRF3.

Figure S4 – related to Figure 3: Loss of ZNRF3 results in proliferative expansion of the zF. This figure is an extended version of Figure 3 from the main manuscript, which includes IHC and proliferation data for *Rnf43* cKO and dKO mice as compared to control and *Znrf3* cKO mice.

Figure S5 – related to Figure 3: Female *Znrf3* cKO mice maintain X-zone marker expression. This figure shows qPCR data for X-zone markers in whole adrenals from 6-week-old control and *Znrf3* cKO mice demonstrating that X-zone cells are still present in *Znrf3* cKOs.

Figure S6 – related to Figure 3: Developmental analysis of *Znrf3* cKO mice. This figure shows IHC for SF1 and TH in control and *Znrf3* cKO mice at P0, P14, and 6 weeks of age demonstrating that the adrenal cortex is increased at birth and continues to expand over time.

Figure S7 – related to Figure 3: SF1-Cre-driven loss of ZNRF3 does not affect corticotrophs in the anterior pituitary. This figure provides histology and lineage tracing in the pituitary to exclude a potential contribution of ZNRF3 loss in the pituitary to the phenotype observed in SF1-Cre-driven cKO mice.

Figure S8 – related to Figure 4: X-zone marker staining in AS-Cre-driven *Znrf3* cKO mice. This figure shows IHC for 20αHSD in 15- and 30-week-old control and *Znrf3* cKO mice demonstrating a progressive expansion of the cortex with loss of ZNRF3 that disrupts the X-zone.

Figure S9 – related to Figure 5: SF1-Cre-mediated loss of PORCN has little effect on adrenocortical zonation and proliferation. This figure shows IHC for zonal markers and proliferation data in 6-week-old male control and *Porcn* cKO mice.

Figure S10 – related to Figure 5: Loss of ZNRF3 results in increased Wnt ligand expression in the inner adrenal cortex. This figure shows single-molecule ISH data for *Wnt5a* in SF1-Cre-driven cKO mice and *Wnt4* in AS-Cre-driven cKO mice, which are both increased in the inner cortex with loss of ZNRF3.

Figure S11 – related to Figure 6: Loss of ZNRF3 results in increased *Axin2* expression in the inner adrenal cortex. This figure shows single-molecule ISH data for *Axin2* in 52-week-old AS-Cre-driven cKO mice and confirms results obtained with SF1-Cre.

Figure S12 – related to Figure 6: *AXIN2* is expressed along a gradient in the normal human adrenal cortex. This figure shows single-molecule ISH for *AXIN2* in a normal human adrenal gland in which *AXIN2* expression gradually decreases from the outer to inner cortex.

Figure S13 – related to Figure 7: Reduced β-catenin dosage significantly reverses the ZNRF3-deficient phenotype. This figure shows normalized adrenal weights for male cKO mice, which confirm results in female cKO mice.

Figure S14 – related to Figures 2, 4, 5, and 7: Loss of RNF43 and/or ZNRF3 in the adrenal cortex does not alter body weight. This figure provides mouse body weights for each genetic model that was generated and demonstrates that body weight is unchanged.

Figure S15 – related to Figures 1, 5, and 6: Quantification of single-molecule ISH data based on pixel area. This figure provides example images to demonstrate how quantification of ISH data was performed.

Table S1 – complete list of qPCR primers, single-molecule ISH probes, and antibodies.

Table S2 – complete list of statistical information including sample sizes, exact P-values, t-values and degrees of freedom (t-test), and F values and degrees of freedom (ANOVA).

Additional Methods – description of additional methods used.

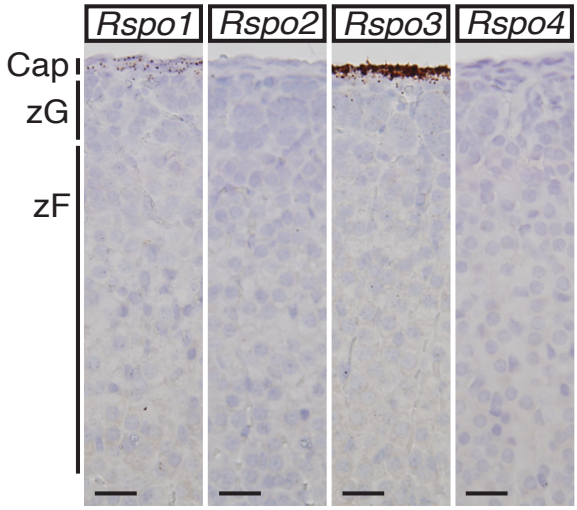

Supplemental Figure 1. *Rspo3* from the outer adrenal capsule is the main source of R-spondins in the adrenal gland. Representative images of single-molecule ISHs from 6-week-old female mice are shown. Scale bars, 25 μm. Abbreviations: Cap, capsule; zG, zona glomerulosa; zF, zona fasciculata.

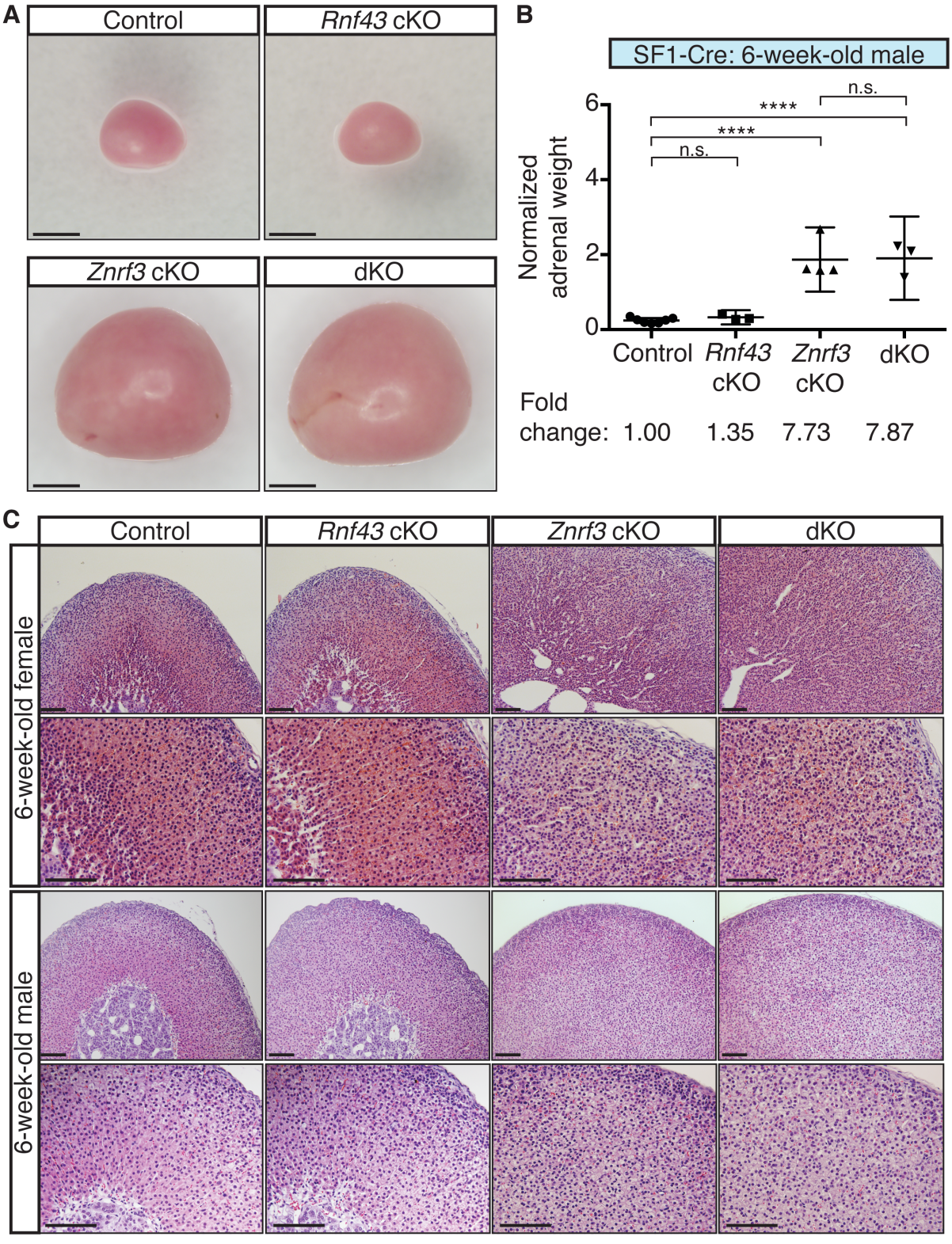
A
Control
Rnf43 cKO
Znrf3 cKO
dKO
B
SF1-Cre: 6-week-old male
Normalized adrenal weight
6
4
2
0
n.s.
****
****
n.s.
Control
Rnf43 cKO
Znrf3 cKO
dKO
Fold change: 1.00 1.35 7.73 7.87
C
Control
Rnf43 cKO
Znrf3 cKO
dKO
6-week-old female
6-week-old male

Supplemental Figure 2. Male *Znrf3* cKO mice are histologically similar to female cKOs. (A) Whole adrenal glands from male *Znrf3* cKO and *Rnf43*;*Znrf3* dKO mice are significantly larger in size at 6 weeks of age compared to control or *Rnf43* cKO mice. Scale bar, 1 mm. (B) Normalized adrenal weights shown as mean and 95% CI. Statistical analysis was performed using one-way ANOVA followed by Tukey's *post hoc* test; ****$p<0.0001$. (C) Loss of *Znrf3* in both female and male mice disrupts normal adrenocortical architecture. Scale bars, 100 μm.

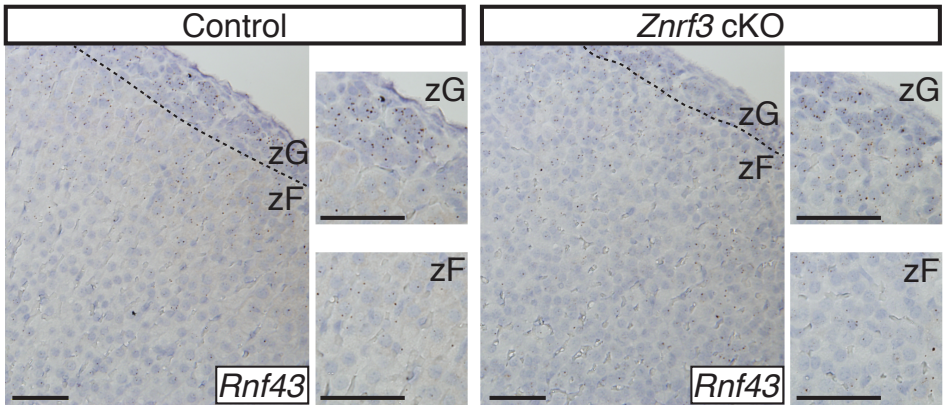

Supplemental Figure 3. *Rnf43* does not compensate for *Znrf3* loss in the adrenal cortex. Consistent with a lack of functional compensation, *Rnf43* expression is not induced in response to *Znrf3* loss. Representative images from single-molecule ISHs performed on adrenal glands isolated from 6-week-old female mice are shown. Dashed line marks histological zG/zF boundary. Scale bars, 50 μm. Abbreviations: zG, zona glomerulosa; zF, zona fasciculata.

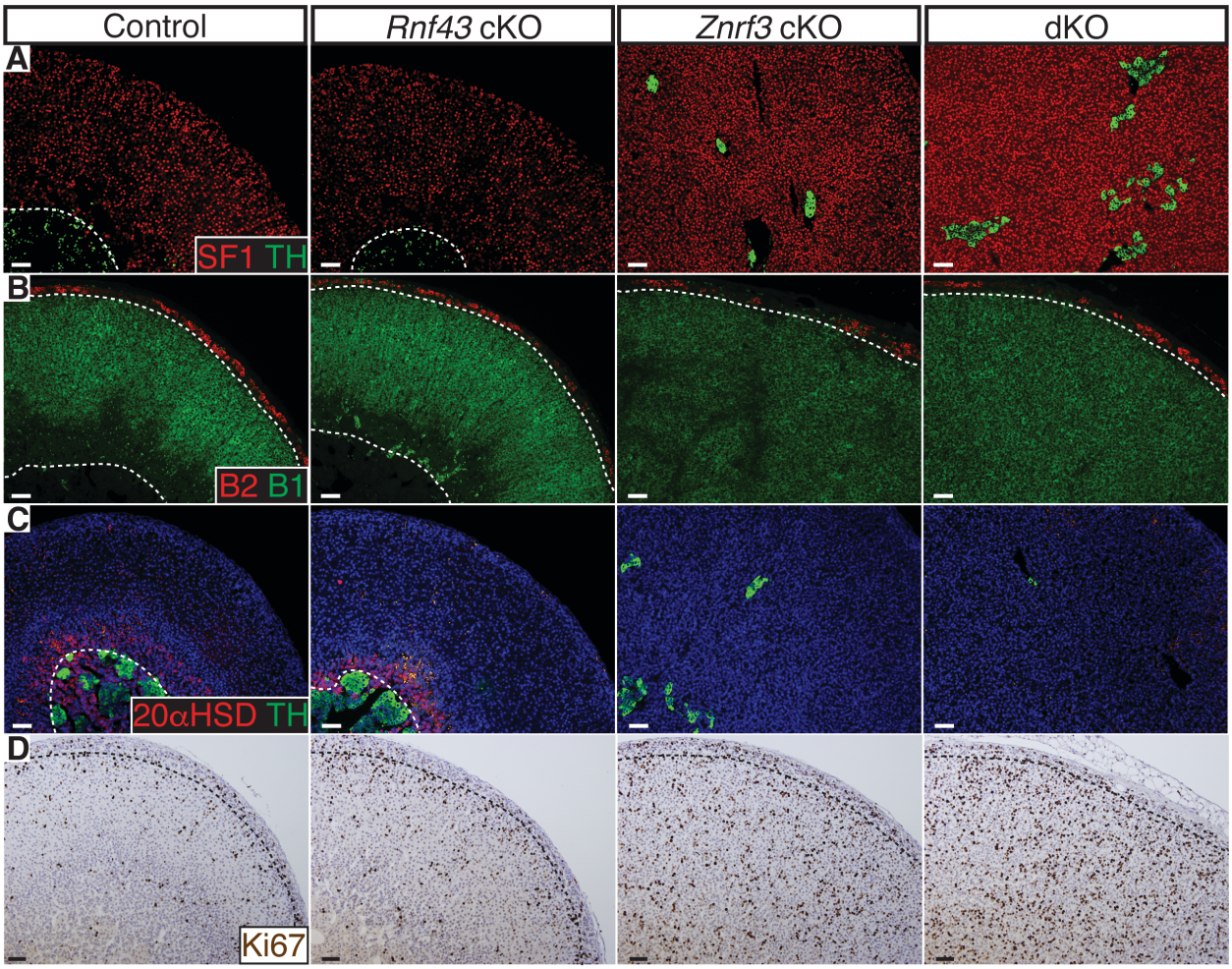
Control
Rnf43 cKO
Znrf3 cKO
dKO
A
SF1 TH
B
B2 B1
C
20αHSD TH
D
Ki67

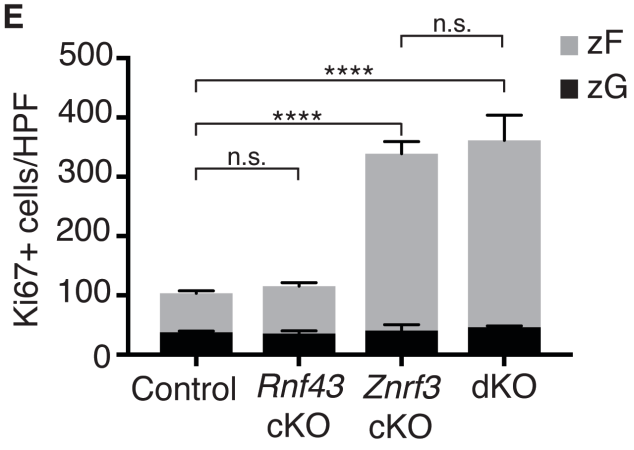
E
Ki67+ cells/HPF
500
400
300
200
100
0
n.s.
****
****
n.s.
zF
zG
Control
Rnf43 cKO
Znrf3 cKO
dKO

Supplemental Figure 4. Loss of ZNRF3 results in proliferative expansion of the zF. (A-C) ZNRF3 loss expands the zF and disrupts organization of the inner adrenal medulla. Dashed lines mark histological cortical/medullary and zG/zF boundaries. (D) ZNRF3 loss significantly increases proliferation in the zF based on IHC for Ki67. (E) Quantification of Ki67 based on the number of positive cells per HPF within the histological zG or zF. Results are shown as mean ± SEM with 3 biological replicates per genotype. Statistical analysis was performed using two-way ANOVA followed by Tukey's *post hoc* test; ****p<0.0001. Reported statistical results represent comparison between zF compartments (gray bars). No significant differences were observed between zG compartments (black bars). All data shown is from female mice. Scale bars, 50 μm. Abbreviations: SF1, steroidogenic factor 1; TH, tyrosine hydroxylase; B2, aldosterone synthase; B1, 11β-hydroxylase; 20αHSD, 20α-hydroxysteroid dehydrogenase; HPF, high power field; zG, zona glomerulosa; zF, zona fasciculata.

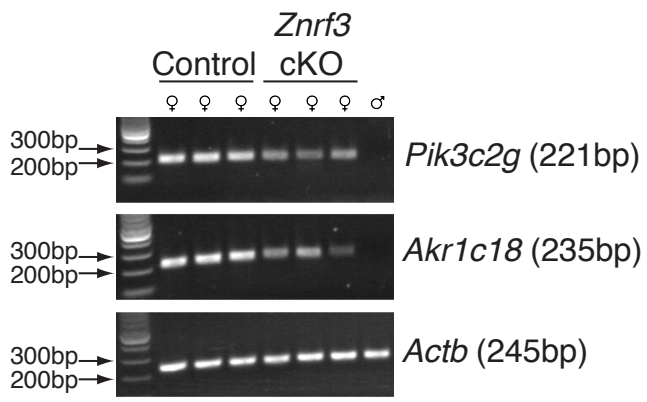

Supplemental Figure 5. Female *Znrf3* cKO mice maintain X-zone marker expression. Expression of the X-zone markers, *Pik3c2g* and *Akr1c18*, is maintained in 6-week-old female *Znrf3* cKO mice as compared to 6-week-old male mice, which have undergone X-zone regression. Gene expression was measured by qPCR in 3 independent control or *Znrf3* cKO mice and analyzed by gel electrophoresis. β-actin (*Actb*) was measured as an internal reference gene.

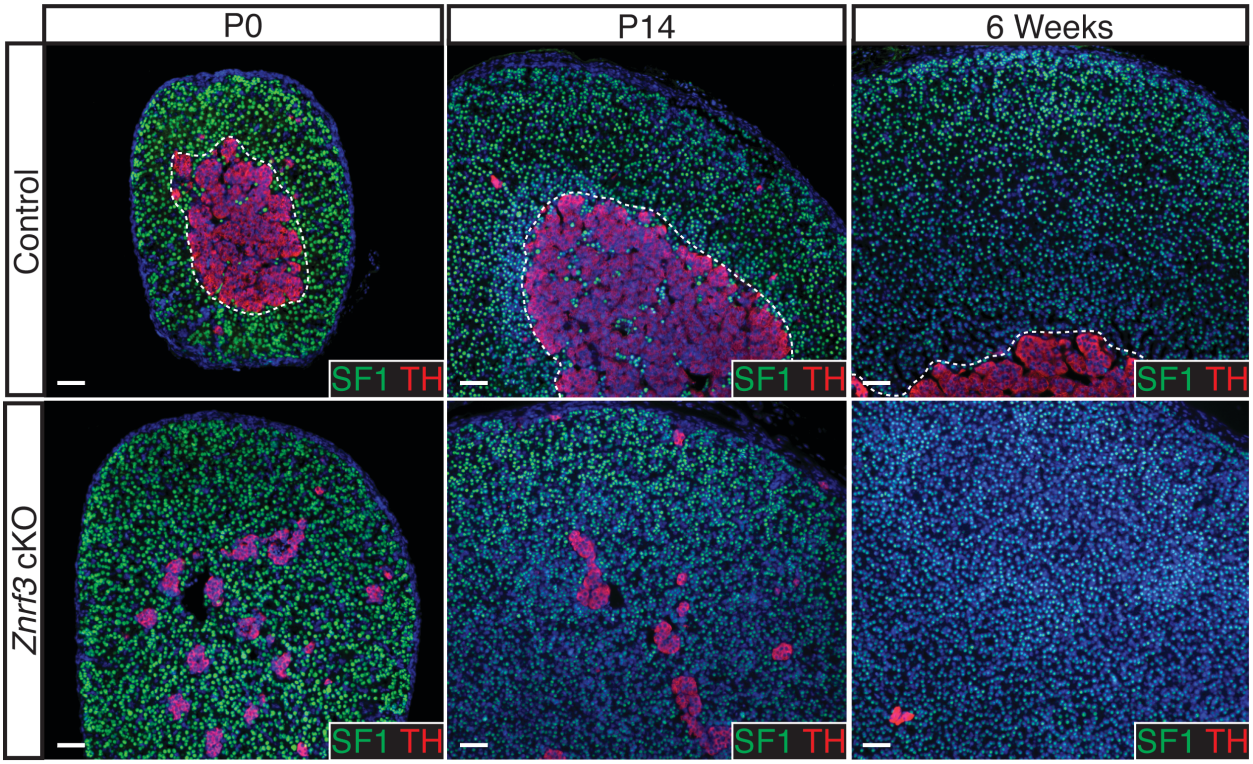

Supplemental Figure 6. Developmental analysis of *Znrf3* cKO mice. SF1-Cre-mediated loss of ZNRF3 results in expansion of the adrenal cortex as early as P0. IHC for SF1 (cortical cell marker) and TH (medulla cell marker) in female mice is shown. DAPI marks nuclei and dashed line marks histological cortical/medullary boundary. Scale bars, 50 μm. Abbreviations: SF1, steroidogenic factor 1; TH, tyrosine hydroxylase.

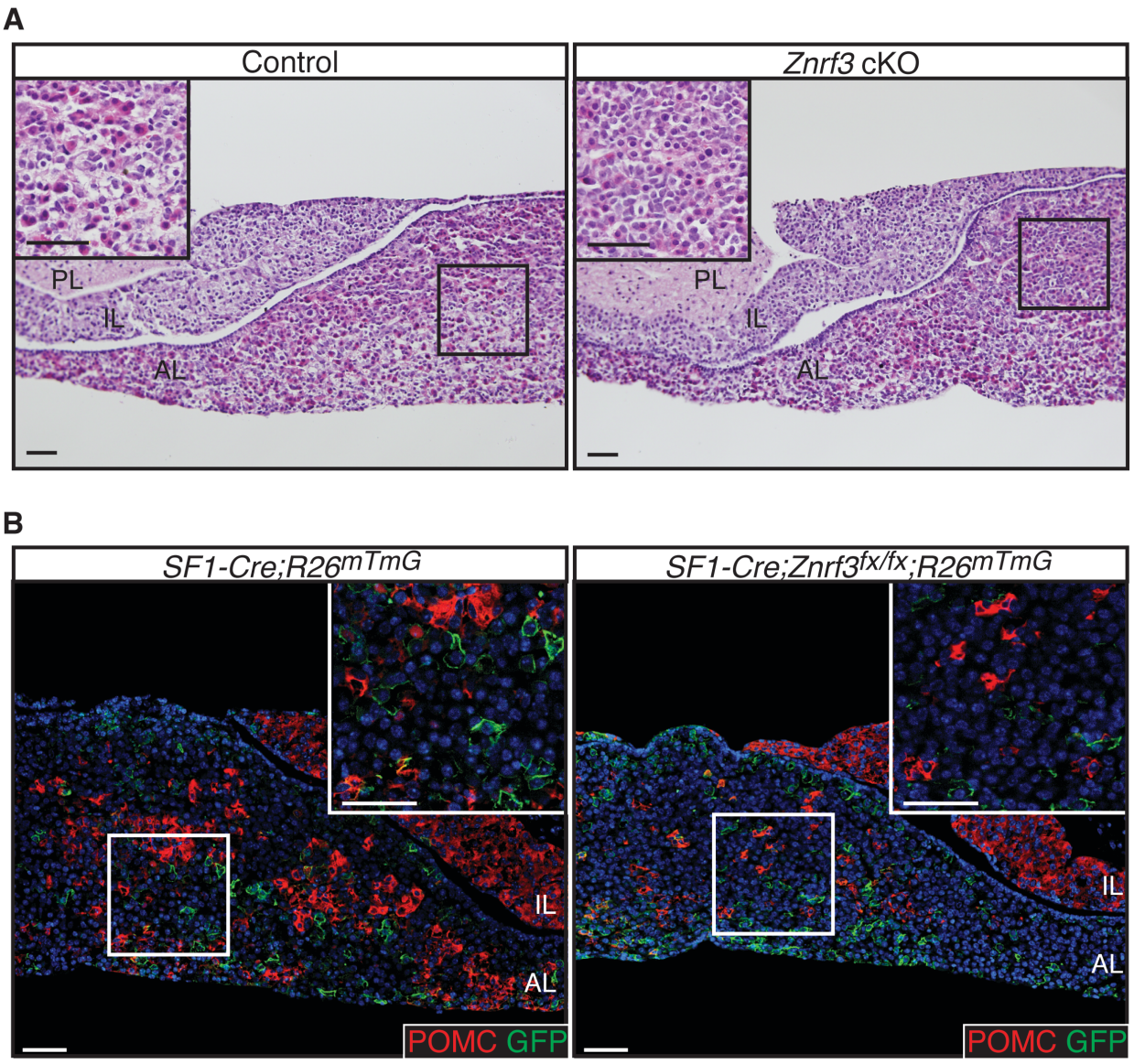

Supplemental Figure 7. SF1-Cre-driven loss of ZNRF3 does not affect corticotrophs in the anterior pituitary. (A) Histological analysis of pituitaries collected from 6-week-old female control or *Znrf3* cKO mice. (B) Lineage tracing in SF1-Cre mice crossed to the mT/mG reporter mouse ($R26^{mTmG}$) shows that Cre recombination does not occur in corticotrophs, which are located in the anterior pituitary and marked by POMC expression. DAPI marks nuclei. Scale bars, 50 μm. Abbreviations: PL, posterior lobe; IL, intermediate lobe; AL, anterior lobe; POMC, pro-opiomelanocortin.

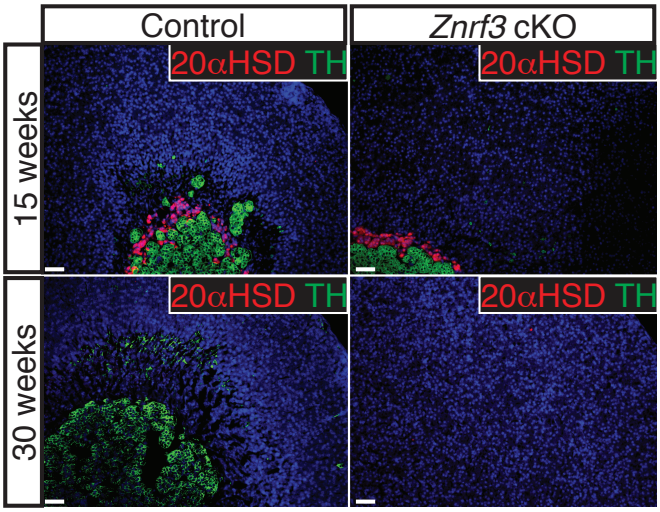

Supplemental Figure 8. X-zone marker staining in AS-Cre-driven *Znrf3* cKO mice. Staining for 20αHSD (X-zone) and TH (medulla) shows that loss of ZNRF3 results in progressive expansion of the cortex, which disrupts the X-zone and medulla by 30 weeks of age. DAPI marks nuclei. Scale bars, 50 μm. Abbreviations: 20αHSD, 20α-hydroxysteroid dehydrogenase; TH, tyrosine hydroxylase.

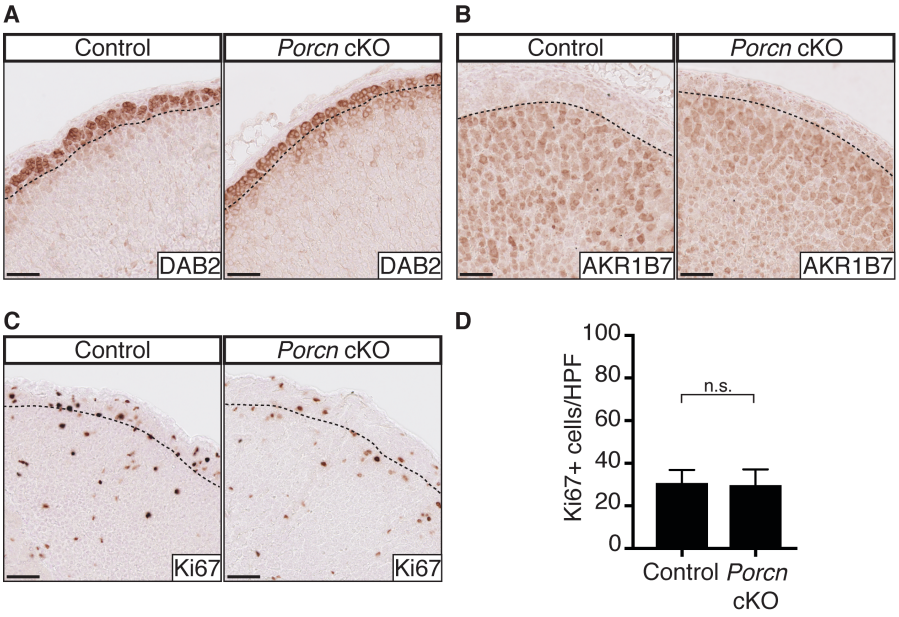

Supplemental Figure 9. SF1-Cre-mediated loss of PORCN has little effect on adrenocortical zonation and proliferation. (A) DAB2 (zG) and (B) AKR1B7 (zF) staining in 6-week-old male control and *Porcn* cKO mice shows only a mild increase in AKR1B7 with loss of PORCN. (C-D) Proliferation, as measured by IHC for Ki67, is unchanged between control and *Porcn* cKOs. Quantification of Ki67 based on the number of positive cells per HPF. Results are shown as mean ± SEM with 6 biological replicates per genotype. Statistical analysis was performed using two-tailed Student's t-test. Dashed lines mark histological zG/zF boundaries. Scale bars, 50 μm. Abbreviations: DAB2, disabled-2; AKR1B7, aldo-keto reductase family 1, member B7; HPF, high power field.

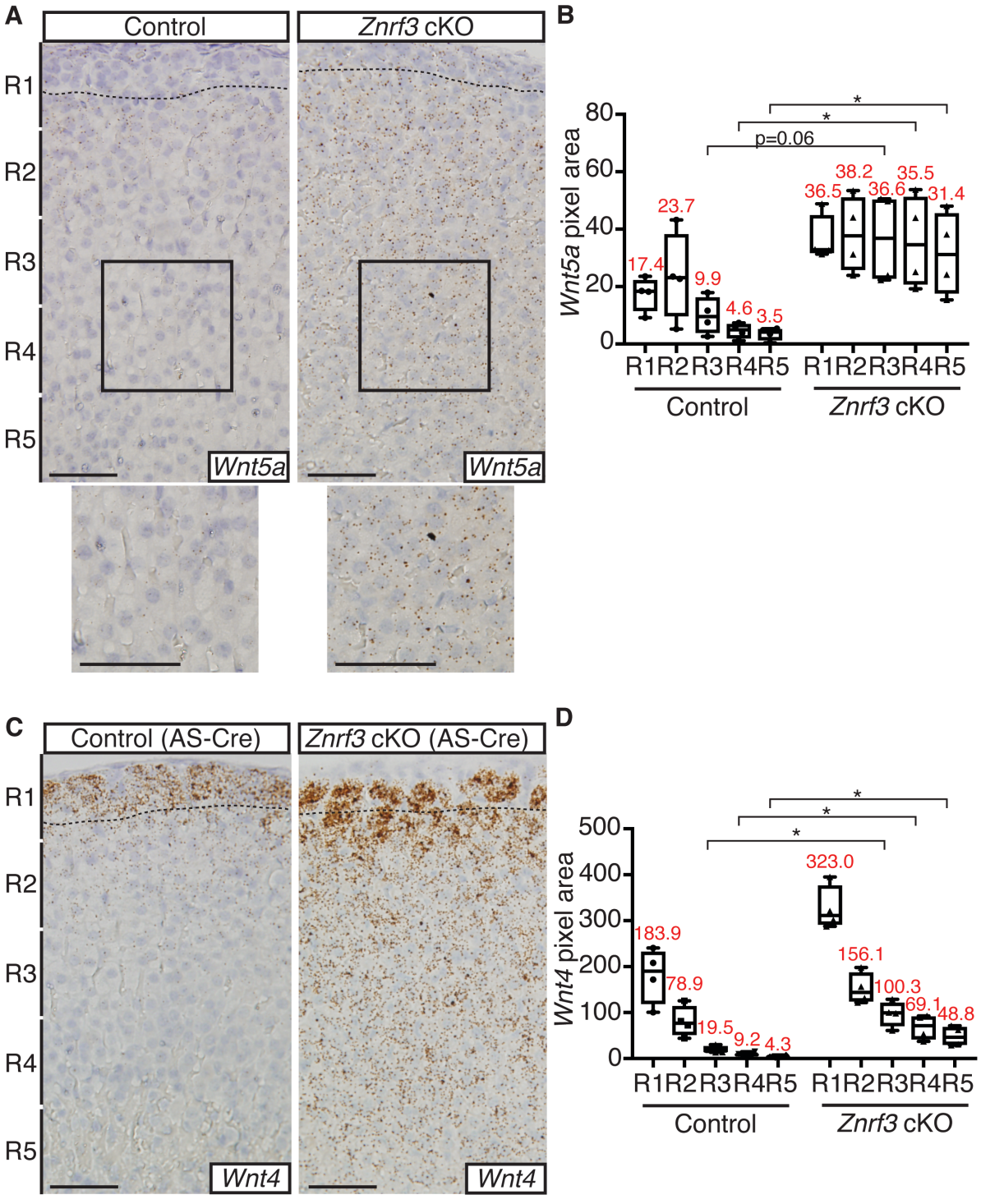
A
Control
Znrf3 cKO
R1
R2
R3
R4
R5
Wnt5a
Wnt5a
B
Wnt5a pixel area
80
60
40
20
0
p=0.06
*
*
*
17.4
23.7
9.9
4.6
3.5
36.5
38.2
36.6
35.5
31.4
R1R2R3R4R5
R1R2R3R4R5
Control
Znrf3 cKO
C
Control (AS-Cre)
Znrf3 cKO (AS-Cre)
R1
R2
R3
R4
R5
Wnt4
Wnt4
D
Wnt4 pixel area
500
400
300
200
100
0
*
*
*
183.9
78.9
19.5
9.2
4.3
323.0
156.1
100.3
69.1
48.8
R1R2R3R4R5
R1R2R3R4R5
Control
Znrf3 cKO

Supplemental Figure 10. Loss of ZNRF3 results in increased Wnt ligand expression in the inner adrenal cortex. (A) *Wnt5a* is significantly increased in the inner cortex of *Znrf3* cKOs. Single-molecule ISHs were performed in 6-week-old female SF1-Cre-driven cKOs. Dashed line marks histological zG/zF boundary. Scale bars, 50 μm. (B) Quantification of *Wnt5a* ISH data based on pixel area within 5 equal sized regions (R1-R5) extending from the outer capsule. Results are shown as mean ± SEM with 4 biological replicates per genotype. Mean pixel area for each region is noted in red. Statistical analysis was performed using one-way ANOVA followed by Tukey's *post hoc* test; *p<0.05. (C) As observed with SF1-Cre, *Wnt4* is expressed along a gradient in the normal adrenal cortex and significantly increased in the inner cortex of AS-Cre-driven cKOs. Single-molecule ISHs were performed in 52-week-old females. Dashed line marks histological zG/zF boundary. Scale bars, 50 μm. (D) Quantification of *Wnt4* ISH data based on pixel area within 5 equal sized regions (R1-R5) extending from the outer capsule. Results are shown as mean ± SEM with 4 biological replicates per genotype. Mean pixel area for each region is noted in red. Statistical analysis was performed using one-way ANOVA followed by Tukey's *post hoc* test; *p<0.05. Abbreviations: AS, aldosterone synthase.

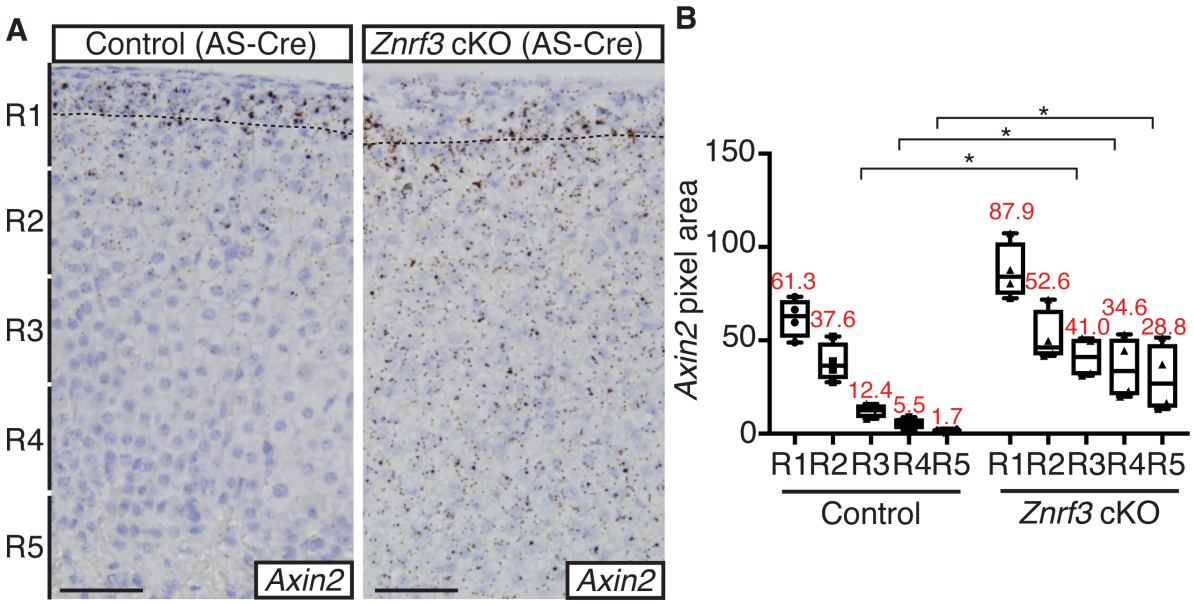

Supplemental Figure 11. Loss of ZNRF3 results in increased *Axin2* expression in the inner adrenal cortex. AS-Cre-driven loss of ZNRF3 increases *Axin2* expression in the zF. (A) Representative images from 52-week-old females are shown. Dashed line marks histological zG/zF boundary. Scale bars, 50 μm. (B) *Axin2* quantification based on pixel area within 5 equal sized regions (R1-R5) extending from the outer capsule. Results are shown as mean ± SEM with 4 biological replicates per genotype. Mean pixel area for each region is noted in red. Statistical analysis was performed using one-way ANOVA followed by Tukey's *post hoc* test; *p<0.05. Abbreviations: AS, aldosterone synthase.

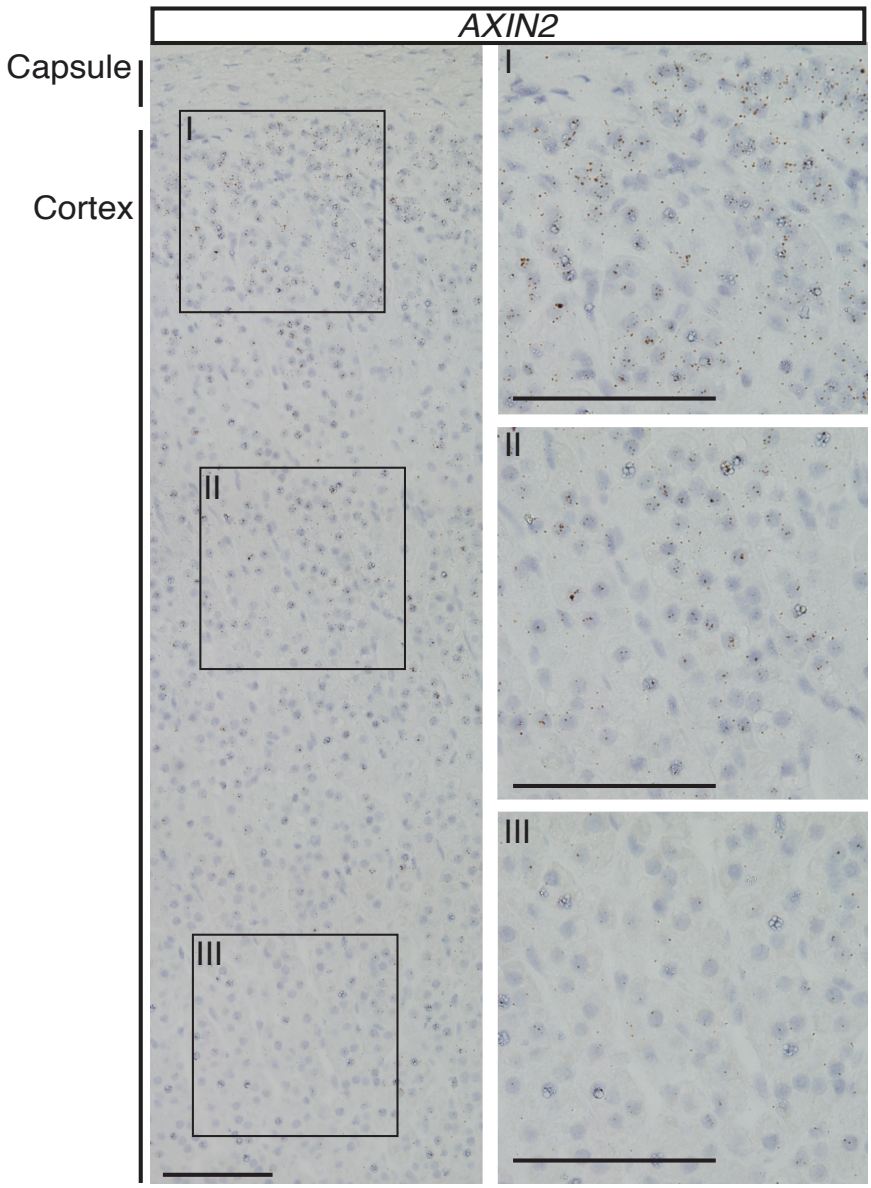

Supplemental Figure 12. *AXIN2* is expressed along a gradient in the normal human adrenal cortex. Single-molecule ISH for *AXIN2* in a normal human adrenal gland. Scale bars, 100 μm.

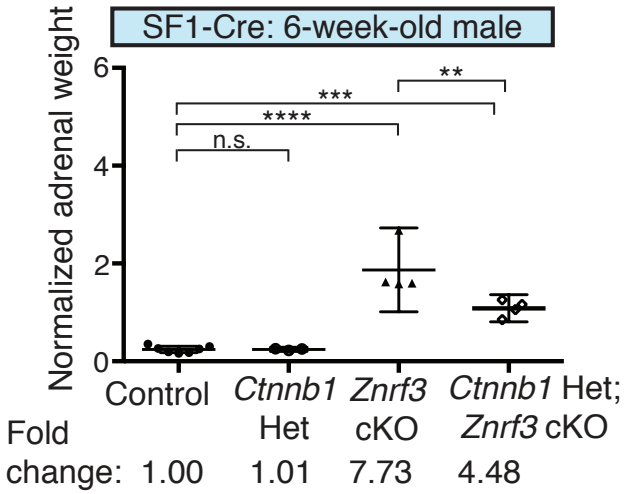

Supplemental Figure 13. Reduced β-catenin dosage significantly reverses the ZNRF3-deficient phenotype. Loss of a single copy of *Ctnnb1* in the context of ZNRF3 loss significantly rescues adrenal weight. Normalized adrenal weights for male cKOs are shown as mean and 95% CI. Statistical analysis was performed using one-way ANOVA followed by Tukey's *post hoc* test; **p<0.01, ***p<0.001, ****p<0.0001. Abbreviations: Het, heterozygous.

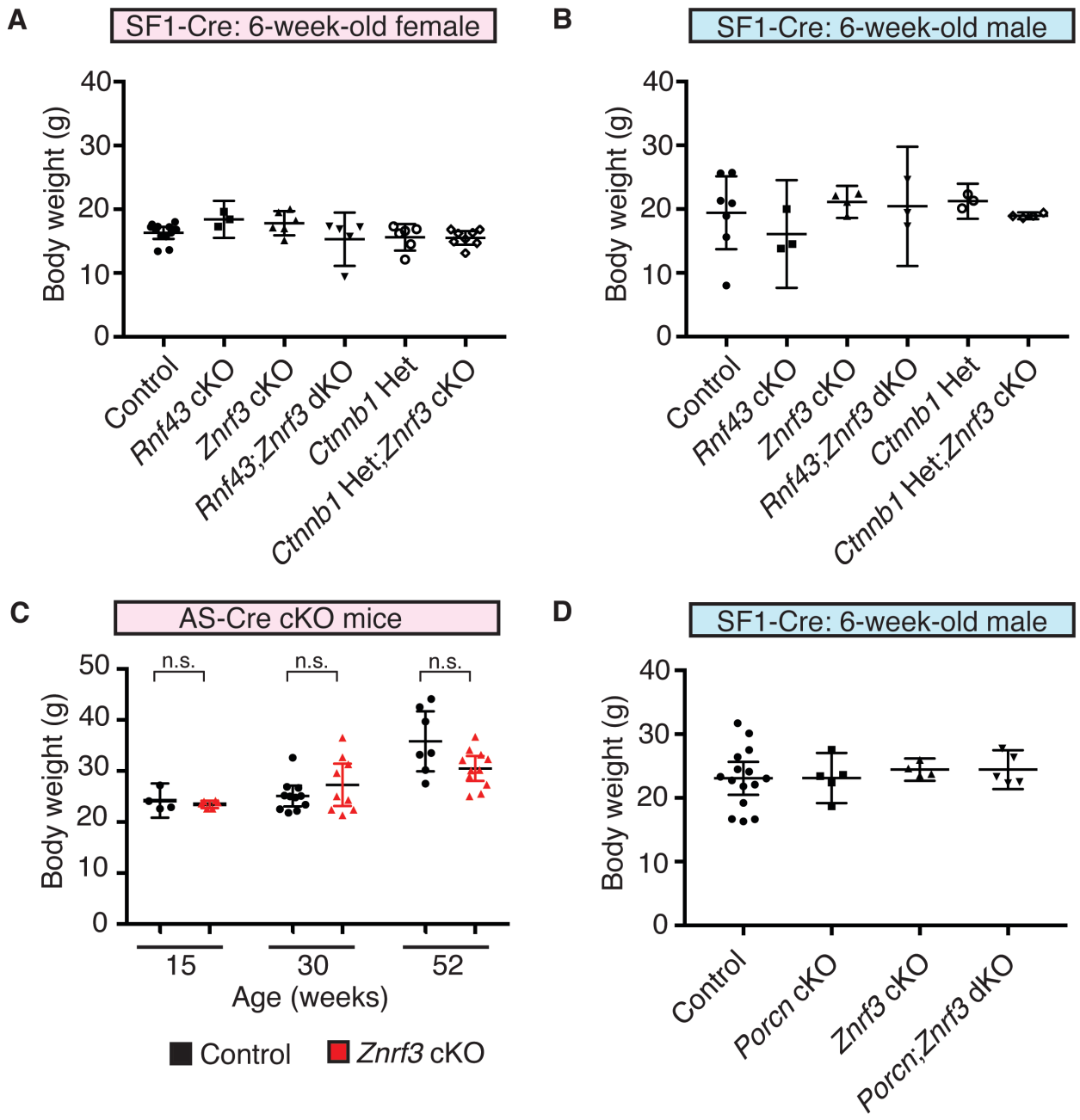

Supplemental Figure 14. Loss of ZNRF3 and/or RNF43 in the adrenal cortex does not alter body weight. Body weights of mice from (A) female SF1-Cre-driven (B), male SF1-Cre-driven, and (C) AS-Cre-driven cKOs are not significantly different between genotypes and are (D) consistent with the independently derived *Porcn* cohort. Results are shown as mean and 95% CI. Statistical analysis was performed using (A-B, D) one-way ANOVA or (C) two-tailed Welch's t-test. Abbreviations: SF1, steroidogenic factor 1; AS, aldosterone synthase; Het, heterozygous.

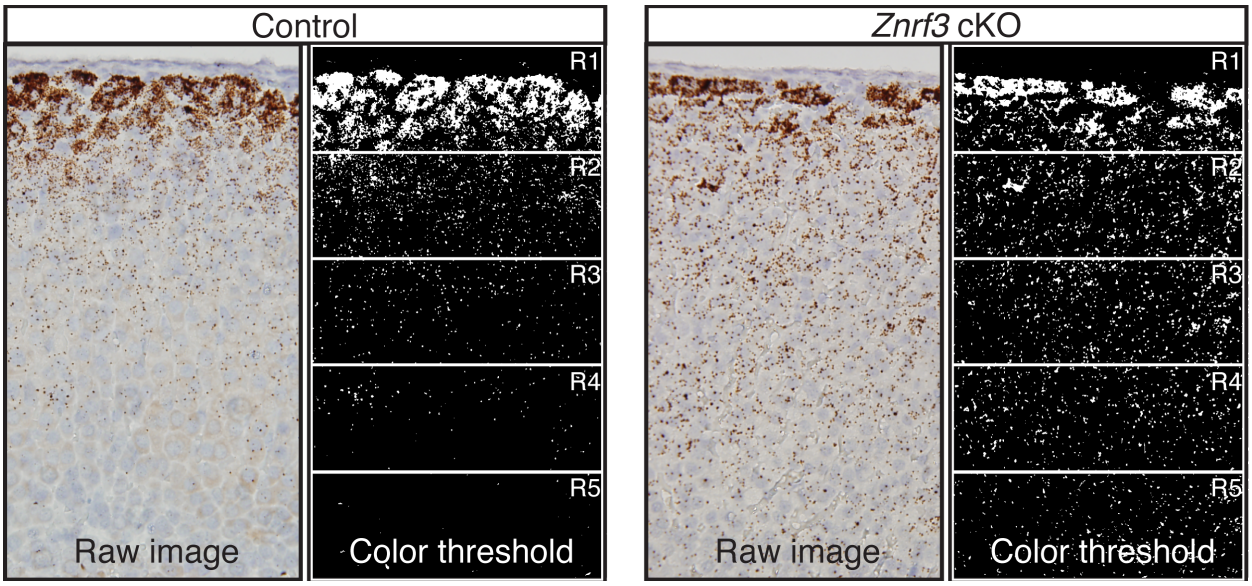

Supplemental Figure 15. Quantification of single-molecule ISH data based on pixel area. Example images of single-molecule ISHs and quantification based on pixel area. Images acquired at 40X magnification were analyzed using ImageJ and the "color threshold" function for hue, saturation, and brightness. Pixel area was measured within 5 equal sized regions of interest (R1-5) extending from the outer capsule. The first region was defined based on the average size of the histological zG across all images (200 pixels in height). The remaining cortex was then divided into equivalent regions (5 regions in total) and quantified based on pixel area. At least 3 images were analyzed per sample and at least 3 biological replicates were analyzed per genotype.

Supplementary Table 1

Primers used for qPCR

Gene	Forward primer (5'->3')	Reverse primer (5'->3')
β-actin	GTGACGTTGACATCCGTAAAGA	GCCGGACTCATCGTACTCC
Pik3c2g	CCATTTGTGGACCCAGGTGA	GGGTCAGTGCATTTTGGAACA
Akr1c18	GGCTTTGGCACCTATGCAAC	TGGGTCTGACCAACTCTGGA

Probes used for single-molecule ISH

Gene	Source	Probe target region
Polr2a (positive control)	ACD #312471	2802-3678
Dapb (negative control)	ACD #310043	414-862
Rspo1	ACD #401991	550-1679
Rspo2	ACD #402001	537-1452
Rspo3	ACD #402011	731-2164
Rspo4	ACD #402021	1180-2202
Rnf43	ACD #400371	170-1284
Znrf3	ACD #434201	1139-2155
Wnt1	ACD #401091	1204-2325
Wnt2	ACD #313601	857-2086
Wnt2b	ACD #405031	1327-2416
Wnt3	ACD #312241	134-1577
Wnt3a	ACD #405041	683-1615
Wnt4	ACD #401101	2147-3150
Wnt5a	ACD #316791	209-1431
Wnt5b	ACD #405051	319-1807
Wnt6	ACD #401111	780-2026
Wnt7a	ACD #401121	1811-3013
Wnt7b	ACD #401131	1597-2839
Wnt8a	ACD #405061	180-1458
Wnt8b	ACD #405071	2279-3217
Wnt9a	ACD #405081	1546-2495
Wnt9b	ACD #405091	727-1616
Wnt10a	ACD #401061	479-1948
Wnt10b	ACD #401071	989-2133
Wnt11	ACD #405021	818-1643
Wnt16	ACD #401081	453-1635
Axin2 (mouse)	ACD #400331	330-1287
AXIN2 (human)	ACD #400241	502-1674

Antibodies used for IHC

Protein target	Source	Dilution	Antigen retrieval method
CD31	Dianova #DIA-310	1:25	10mM NaCitrate, pH 6.0 + 0.05% Tween-20
GFP	Aves #GFP-1020	1:1000	10mM NaCitrate, pH 6.0 + 0.05% Tween-20
TH	Millipore #MAB318	1:200	10mM NaCitrate, pH 6.0 + 0.05% Tween-20 or 10mM Citric Acid, pH 2.6 + 0.05% Tween-20
SF1	Custom	1:1000	10mM Citric Acid, pH 2.6 + 0.05% Tween-20
CYP11B2	Dr. Celso Gomez-Sanchez	1:200	1mM EDTA, 10mM diethanolamine, pH9
CYP11B1-555	Dr. Celso Gomez-Sanchez	1:100	1mM EDTA, 10mM diethanolamine, pH9
20αHSD	Dr. Yacob Weinstein	1:1000	10mM Citric Acid, pH 2.6 + 0.05% Tween-20
Ki67	Thermo Fisher #MA5-14520	1:200	10mM NaCitrate, pH 6.0 + 0.05% Tween-20
DAB2	BD Transduction Laboratories #610464	1:500	10mM NaCitrate, pH 6.0 + 0.05% Tween-20
Non-phospho (active) β-catenin	Cell Signaling #8814	1:500	10mM NaCitrate, pH 6.0 + 0.05% Tween-20
POMC	National Hormone and Peptide Program	1:150	N/A
AKR1B7	Santa Cruz #SC-27763	1:200	10mM NaCitrate, pH 6.0 + 0.05% Tween-20

Supplementary Table 2

Comprehensive summary of statistical information

Figure	Sample size	Statistical test	t-value and degrees of freedom (t-test) F value and degrees of freedom (ANOVA)	Exact p-value
Figure 1C	*Rnf43*: 4 mice *Znrf3*: 3 mice	two-tailed Student's t-test	t(5) = 3.96	p=0.0107
Figure 1D	*Rnf43*: 3 mice *Znrf3*: 3 mice	two-tailed Student's t-test	t(4) = 3.89	p=0.0177
Figure 2B	Control: 12 mice *Rnf43* cKO: 3 mice *Znrf3* cKO: 6 mice dKO: 5 mice	Welch's one-way ANOVA, Games-Howell *post hoc*	F(3,5.79) = 58.15	p=0.0001
Figure 3F	Control: 3 mice *Znrf3* cKO: 3 mice	two-way ANOVA, Tukey's *post hoc*	genotype: F(1,8) = 102.40 zone: F(1,8) = 150.90 genotype*zone: F(1,8) = 97.56	p<0.0001 p<0.0001 p<0.0001
Figure 3G	Control: 3 mice *Znrf3* cKO: 3 mice	two-way ANOVA, Tukey's *post hoc*	genotype: F(1,8) = 39.97 zone: F(1,8) = 44.57 genotype*zone: F(1,8) = 31.70	p=0.0002 p=0.0002 p=0.0002
Figure 3H	Control: 14 mice *Znrf3* cKO: 8 mice	two-tailed Welch's t-test	t(9.96) = 0.20	p=0.8215
Figure 3I	Control: 11 mice *Znrf3* cKO: 10 mice	two-tailed Welch's t-test	t(13.25) = 4.05	p=0.0013
Figure 4C	15 week Control: 4 mice 15 week *Znrf3* cKO: 6 mice 30 week Control: 11 mice 30 week *Znrf3* cKO: 9 mice 52 week Control: 7 mice 52 week *Znrf3* cKO: 11 mice	two-tailed Student's t-test two-tailed Welch's t-test two-tailed Welch's t-test	t(8) = 2.26 t(8.23) = 4.43 t(10.06) = 6.37	p=0.0535 p=0.0021 p<0.0001
Figure 4F	15 week Control: 3 mice 15 week *Znrf3* cKO: 4 mice 30 week Control: 5 mice 30 week *Znrf3* cKO: 7 mice 52 week Control: 5 mice 52 week *Znrf3* cKO: 5 mice	two-way ANOVA, Tukey's *post hoc* two-way ANOVA, Tukey's *post hoc* two-way ANOVA, Tukey's *post hoc*	genotype: F(1,10) = 0.040 zone: F(1,10) = 35.69 genotype*zone: F(1,10) = 0.11 genotype: F(1,20) = 10.85 zone: F(1,20) = 58.41 genotype*zone: F(1,20) = 9.67 genotype: F(1,16) = 16.48 zone: F(1,16) = 38.31 genotype*zone: F(1,16) = 12.41	p=0.8448 p=0.0001 p=.7505 p=0.0036 p<0.0001 p=0.0055 p=0.0009 p<0.0001 p=0.0028
Figure 5A	Control: 15 mice *Porcn* cKO: 5 mice *Znrf3* cKO: 4 mice dKO: 5 mice	one-way ANOVA, Tukey's *post hoc*	F(3,25) = 7.74	p<0.0001
Figure 5D	Control: 5 mice *Znrf3* cKO: 5 mice	one-way ANOVA, Tukey's *post hoc*	F(9,40) = 56.55	p<0.0001 p<0.0001
Figure 6C	Control: 4 mice *Znrf3* cKO: 4 mice	one-way ANOVA, Tukey's *post hoc*	F(9,30) = 44.77	p<0.0001
Figure 6D	zG: 3 samples zF: 3 samples zR: 3 samples	one-way ANOVA, Tukey's *post hoc*	F(2,6) = 54.88	p=0.0001
Figure 7A	None: 46 tumor samples *CTNNB1*: 12 tumor samples *ZNRF3*: 17 tumor samples	Welch's one-way ANOVA, Games-Howell *post hoc*	F(2,36.53) = 78.98	p<0.0001
Figure 7B	Control: 12 mice *Ctnnb1* Het: 6 mice *Znrf3* cKO: 6 mice *Ctnnb1* Het;*Znrf3* cKO: 8 mice	Welch's one-way ANOVA, Games-Howell *post hoc*	F(3,11.92) = 63.21	p<0.0001
Figure 7C	Control: 3 mice *Ctnnb1* Het: 3 mice *Znrf3* cKO: 3 mice *Ctnnb1* Het;*Znrf3* cKO: 3 mice	two-way ANOVA, Tukey's *post hoc*	genotype: F(3,20) = 39.41 zone: F(1,20) = 146.4 genotype*zone: F(3,20) = 33.45	p<0.0001 p<0.0001 p<0.0001
Supplemental figure 2B	Control: 7 mice *Rnf43* cKO: 3 mice *Znrf3* cKO: 4 mice dKO: 3 mice	one-way ANOVA, Tukey's *post hoc*	F(3,13) = 35.61	p<0.0001
Supplemental figure 4E	Control: 3 mice *Rnf43* cKO: 3 mice *Znrf3* cKO: 3 mice dKO: 3 mice	two-way ANOVA, Tukey's *post hoc*	genotype: F(3,16) = 32.26 zone: F(1,16) = 149 genotype*zone: F(3,16) = 28.6	p<0.0001 p<0.0001 p<0.0001
Supplemental figure 9D	Control: 6 mice *Porcn* cKO: 6 mice	two-tailed Student's t-test	t(10) = 0.11	p=0.9174
Supplemental figure 10B	Control: 4 mice *Znrf3* cKO: 4 mice	one-way ANOVA, Tukey's post hoc	F(9,30) = 6.01	p<0.0001
Supplemental figure 10D	Control: 4 mice *Znrf3* cKO: 4 mice	one-way ANOVA, Tukey's post hoc	F(9,30) = 38.20	p<0.0001
Supplemental figure 11B	Control: 4 mice *Znrf3* cKO: 4 mice	one-way ANOVA, Tukey's post hoc	F(9,30) = 20.32	p<0.0001
Supplemental figure 13	Control: 7 mice *Ctnnb1* Het: 3 mice *Znrf3* cKO: 4 mice *Ctnnb1* Het;*Znrf3* cKO: 4 mice	one-way ANOVA, Tukey's *post hoc*	F(3,14) = 37.66	p<0.0001
Supplemental figure 14A	Control: 12 mice *Rnf43* cKO: 3 mice *Znrf3* cKO: 6 mice *Rnf43*;*Znrf3* dKO: 5 mice *Ctnnb1* Het: 6 mice *Ctnnb1* Het;*Znrf3* cKO: 8 mice	one-way ANOVA	F(5,34) = 2.29	p=0.0671
Supplemental figure 14B	Control: 7 mice *Rnf43* cKO: 3 mice *Znrf3* cKO: 4 mice *Rnf43*;*Znrf3* dKO: 3 mice *Ctnnb1* Het: 3 mice *Ctnnb1* Het;*Znrf3* cKO: 4 mice	one-way ANOVA	F(5,18) = 0.72	p=0.6172
Supplemental figure 14C	15 week Control: 4 mice 15 week *Znrf3* cKO: 6 mice 30 week Control: 11 mice 30 week *Znrf3* cKO: 9 mice 52 week Control: 7 mice 52 week *Znrf3* cKO: 11 mice	two-tailed Welch's t-test two-tailed Welch's t-test two-tailed Welch's t-test	t(3.45) = 0.67 t(11.98) = 1.08 t(8.56) = 2.02	p=0.5432 p=0.3035 p=0.0759
Supplemental figure 14D	Control: 15 mice *Porcn* cKO: 5 mice *Znrf3* cKO: 4 mice *Porcn*;*Znrf3* dKO: 5 mice	one-way ANOVA	F(3,25) = 0.2556	p=0.8566

Additional Methods

Quantitative PCR

Whole adrenals were disrupted for 30 seconds in RLT buffer containing β-mercaptoethanol (Qiagen) using the BeadBug Microtube Homogenizer (Benchmark Scientific) and Lysing Matrix D (MP Bioproducts). RNA was isolated using the RNeasy Mini Plus Kit (Qiagen) and 1 μg total RNA was DNase I treated (Qiagen) and converted to cDNA using the High Capacity cDNA Reverse Transcription Kit (Applied Biosystems) according to manufacturer's instructions. Quantitative PCR was carried out using 5 ng cDNA with the primers listed in Supplemental Table 1 and Power SYBR Green reagent (Applied Biosystems) on an Applied Biosystems QuantStudio 3 Real-Time PCR System. β-actin was used as an internal reference gene.

Pituitary Isolation and Histology

Pituitaries were fixed in 4% paraformaldehyde for 1 hr at 4^{o}C, paraffin embedded, and cut into 5 μm sections. For POMC and GFP co-staining, POMC was detected first without unmasking using HRP-polymer solution (Vector Labs) and Alexa Fluor Tyramide Reagent (Thermo Fisher). Slides were then unmasked and GFP was detected with Dylight-conjugated secondary antibody (Jackson ImmunoResearch, 1:800). Images were acquired on a Nikon A1 galvano laser scanning confocal on a Nikon Eclipse TiE inverted microscope with 4 normal PMT detectors. Images were acquired using a 20X PlanApo lambda (oil immersion, 0.75NA) or 40X PlanApo lambda (oil immersion, 0.95NA) objective.

Human Tissue for Single-Molecule ISH

Formalin-fixed paraffin-embedded (FFPE) adrenal tissue from a de-identified human patient was used for single-molecule ISH as described. Tissue was obtained from a collection of healthy kidney donors at the University of Michigan.

Hormone Measurements

Plasma corticosterone concentrations were determined by liquid-chromatography-tandem mass spectrometry (LC-MS/MS) as follows: a 60 µL aliquot of plasma was mixed with 60 µL internal standard deuterated corticosterone (corticosterone-D8, C/D/N Isotopes) solution (200 ng/dL in methanol: deionized water, 4:6), and 280 µL deionized water. The mixture was loaded on ISOLUTE supported liquid extraction columns (Biotage) and the columns were then washed twice with 0.7 mL methyl-tert-butyl ether (MTBE). The eluent was concentrated under nitrogen and the dried extract was reconstituted with 60 µL of methanol/deionized water (4:6) and transferred to a 0.25 mL vial insert. Samples (10 µL) were injected via autosampler and resolved with a two dimensional chromatography method via a C4, 10 x 2.1 mm column (Restek) on a Agilent 1260 binary pump HPLC, and a Kinetex 50 x 2.1 mm, 2.5 m particle size biphenyl column (Phenomenex) on an Agilent 1290 binary pump, using gradient elution with 0.2 mmol/L ammonium fluoride and methanol. The column effluent was directed into the source of an Agilent 6495 triple quadrupole mass spectrometer using electrospray ionization in positive ionization mode and analyzed using multiple reaction monitoring (MRM) mode. Quantitation was accomplished by comparing ion currents for the monitored ions with 13-point quadratic external calibration curves (R^2 was minimum 0.995) and corrected for recovery of internal standard using ChemStation and MassHunter software (Agilent). Intra-assay and inter-assay coefficients of variability for corticosterone were 3.1% and 8.2%, respectively. The lower limit of detection, defined as the minimum concentration achieving an extrapolated signal-to-noise ratio of 3, was 0.1 ng/dL.